Geomechanics and Engineering, *Vol. 31, No. 5 (2022) 477-488*
https://doi.org/10.12989/gae.2022.31.5.477

Effects of inclined bedrock on dissimilar pile composite foundation under vertical loading

Kaiyu Jiang[1,2,3], Weiming Gong[*1,2], Jiang Xu[**4], Guoliang Dai[1,2] and Xia Guo[5]

[1]*Key of Laboratory for RC and PRC Structure of Education Ministry, Southeast University, Nanjing 211189, China*
[2]*School of Civil Engineering, Southeast University, Nanjing 211189, China*
[3]*School of Civil Engineering, Chongqing Three Gorges University, Chongqing, 404100, China*
[4]*College of Civil Science and Engineering, Yangzhou University, Yangzhou, 225000, China*
[5]*Nuclear Industry Huzhou Survey Planning & Design Institute Co., Ltd. , Zhejiang, 313002, China*

(*Received July 4, 2022, Revised November 20, 2022, Accepted November 23, 2022*)

Abstract. Pile composite foundation (PCF) has been commonly applied in practice. Existing research has focused primarily on semi-infinite media having equal pile lengths with little attention given to the effects of inclined bedrock and dissimilar pile lengths. This investigation considers the effects of inclined bedrock on vertical loaded PCF with dissimilar pile lengths. The pile-soil system is decomposed into fictitious piles and extended soil. The Fredholm integral equation about the axial force along fictitious piles is then established based on the compatibility of axial strain between fictitious piles and extended soil. Then, an iterative procedure is induced to calculate the PCF characteristics with a rigid cap. The results agree well with two field load tests of a single pile and numerical simulation case. The settlement and load transfer behaviors of dissimilar 3-pile PCFs and the effects of inclined bedrock are analyzed, which shows that the embedded depth of the inclined bedrock significantly affects the pile-soil load sharing ratios, non-dimensional vertical stiffness N_0/wdE_s, and differential settlement for different length-diameter ratios of the pile l/d and pile-soil stiffness ratio k conditions. The differential settlement and pile-soil load sharing ratios are also influenced by the inclined angle of the bedrock for different k and l/d. The developed model helps better understand the PCF characteristics over inclined bedrock under vertical loading.

Keywords: boundary element method; fictious pile; inclined bedrock; pile composite foundation; vertical loading

1. Introduction

Subsoil is usually an inhomogeneous distribution, and the underlying stratum is generally inclined bedrock. Pile composite foundation (PCF) with dissimilar pile lengths has drawn great attention in engineering and has been widely applied in ground treatments to reduce differential foundation settlement (Qu and Ding 2021, Yu and Zhou 2020, Abdrabbo and El-wakil 2015). For dissimilar PCFs resting on inclined and rough rigid bedrock, the analysis of critical parameters, such as the pile-soil load sharing ratio, total stiffness, and differential settlement, should be more realistic in practice but also more difficult to handle. The settlement control criterion has been extensively adopted for foundation designs in several design specifications and research to date (Zhang and Huang 2018, GB50007- 2011). Therefore, it is imperative to understand the effects of inclined bedrock on the critical parameters of dissimilar PCFs based on elasticity theory.

The performance of PCFs or pile foundation has been achieved primarily from field load tests (Zhang and Gong 2021, Bai and He 2006) and the finite element method (Ma and Mou 2021, Hassona and Moussa 2022, Saeedi and Rasouli 2018) in many engineering cases. However, field data for large composite foundations cannot often be readily obtained. Considering the settlement-based control criterion for foundation designs, many analytical methods based on elasticity theory, such as the shear displacement method (Huang and Liang 2011), load transfer method (Kodikara and Johnston 1994), simplified method (Yang and Zhang 2011, Kitiyodom and Matsumoto 2002), and variational approach (Shen and Chow 2000, 1999), have been used to analyze the behaviors of PCF and piled raft systems. Elastic theory has been gradually developed and summarized as a theoretical analysis system for pile foundation and included in national design codes (JGJ94- 2008). However, the shear displacement method is not directly suitable for composite foundation analyses as variations in the vertical stress to depth are ignored. The elasticity method given by Poulos and Davis (1980) tends to exaggerate interactions between piles. Then, integral equation methods based on the superposition principle (Banerjee and Davies 1978, Liang and Chen 2009, Chen and Song 2011, Liang and Song 2014) and rigorous boundary element method (BEM) (Kuwabara 1989, Butterfield and Banerjee 1971a, b) have been adopted to reasonable account for the enforcement and shielding effects of neighboring piles. It is noted that these existing methods consider horizontal layered or semi-infinite soil stratum conditions (Randolph and Wroth 1979). For dissimilar pile lengths, Wong and Poulos (2005) presented a

∗Corresponding author, Professor
E-mail: wmgong@seu.edu.cn
**Cooperative Corresponding author
E-mail: yzujxu@yzu.edu.cn

ISSN: 2005-307X (Print), 2092-6219 (Online)

simplified method to approximate settlement interaction factors between dissimilar piles. For inclined bedrock, Han and Jiang (2011) investigated the influence of the inclined angle and embedded depth of bedrock on the bearing capacity and settlement of shallow foundations. Fatolahzadeh and Mehdizadeh (2020) obtained a modified bearing capacity equation for shallow foundation on inclined bedrock. The effects of the inclined bedrock on dissimilar PCFs have not been widely considered.

In this paper, the BEM based on elastic theory is established by extending the approach of Muki and Sternberg (1970). The response of vertically loaded PCFs with dissimilar lengths embedded over inclined bedrock is analyzed. First, the pile-soil system is decomposed into fictitious piles and extended soil and divided into *m* square elements based on the pile diameters. The second Fredholm integral equation about axial strain of the fictitious piles is then established considering the compatibility of the axial strain between the fictitious piles and extended soil, which is based on Mindlin's solutions and the superposition principle. After that, the vertical stiffness of each element is obtained by considering the boundary condition of the bedrock position. Finally, an iterative procedure is induced to calculate the PCF characteristics with a rigid cap. Two field load tests of single pile and solutions from previous research are considered to verify the proposed method. Comprehensive parameter analyses considering the influence of the length-diameter ratios of the pile *l/d*, pile-soil stiffness ratios *k* ($k=E_p/E_s$), inclined angle α, and distance between the bedrock and pile bottom Δ are used to estimate the non-dimensional vertical stiffness N_0/wdE_s, differential settlement of pile-soil system, the load sharing ratios of each element. Compared with rigorous approaches, the proposed method is suitable to analyze large PCF embedded inclined bedrock due to its computational efficiency.

2. Analysis method

The proposed method extends the BEM to dissimilar PCFs with a rigid cap embedded over an inclined bedrock. The settlement-based control criterion for foundation design often places the piles and soil in an elastic state under working conditions. Therefore, the following assumptions are made: (1) There is no slippage at the pile-soil interface; (2) only linear elastic properties of the soil are considered; and (3) there are only vertical forces transmitted between the composite foundation and cap under vertical loads.

2.1 Analytical model

The typical PCF composed of *n* ($n=n_1\times n_2$) dissimilar circular piles with diameter *d* embedded over inclined bedrock is shown in Fig. 1. The n_1 and n_2 are the numbers of rows and columns for the pile layout, respectively, *s* is the center-to-center distance of neighboring piles, *B* indicates the clear overhang width of the cap as extended from the outer piles, and E_s and E_p are the Young's moduli of the soil and piles. respectively. Poisson's ratio for the soil

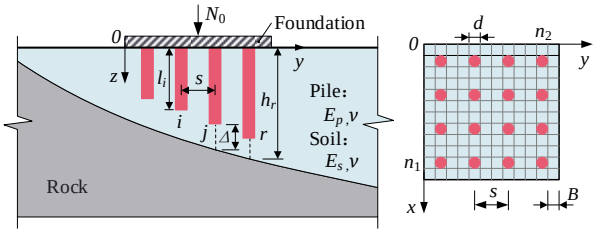

Fig. 1 System of dissimilar PCFs

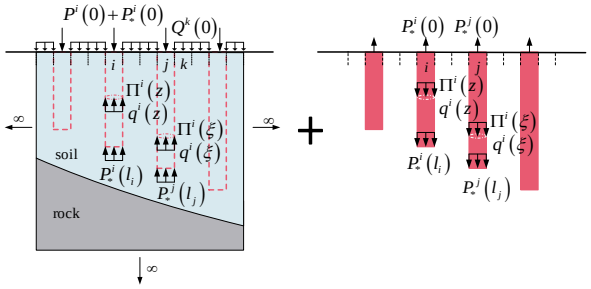

Fig. 2 Decomposition system for the analytical model

and piles are assumed to be the same and equal to *v* to simplify the analysis. The total vertical load is set to N_0.

The composite foundation system is partitioned into *m* square units based on the pile diameter. It is noted that *n* square units are occupied by the pile elements, and the remaining *m-n* square units are the soil elements. The l_i and Δ_i denote the length of pile *i* and the distance between the bedrock and the bottom of pile *i*, and $h_r= l_i+\Delta_i$.

For square units, the vertical loading acting at the *i-th* pile head and *k-th* soil unit head are expressed as $P^i(0)$ and $Q^k(0)$ ($i=1,2,\ldots,n$, $k=n+1,n+2,\ldots,m$), respectively. Following the method proposed by Muki and Sternberg (1970), the pile-soil system is decomposed into extended soil and fictitious piles (Fig. 2). The $P_*^i(z)$ and $q^i(z)$ are the axial force and shaft resistance of the *i-th* fictitious pile at a depth *z*. Then, the load acting at the extended soil is obtained by considering the interaction force between two decomposed systems. For instance, the $P_*^i(0)$ and $P_*^i(l_j)$ are the axial force of the *i-th* fictitious pile head and bottom, and $P^i(0)+P_*^i(0)$ and $Q^k(0)$ are the axial forces of the *i-th* and *k-th* extended soil unit head.

2.2 Fictitious piles

For fictitious piles, the stress-strain equation, equilibrium equation, and strain-displacement relationship of the *i-th* fictitious pile unit are determined based on elasticity theory as follows

$$\varepsilon_*^i(z)=\frac{P_*^i(z)}{E_*A}\quad(0\le z\le l_i,\ i=1,2,\cdots,n) \tag{1}$$

$$\frac{dP_*^i(z)}{dz}=-q^i(z)\quad(0\le z\le l_i,\ i=1,2,\cdots,n) \tag{2}$$

$$\varepsilon_*^i(z)=\frac{dw_*^i(z)}{dz} \quad (0\le z\le l_i,\ i=1,2,\cdots,n) \tag{3}$$

where $\varepsilon_*^i(z)$, $w_*^j(z)$, and A denote the axial strain and settlement at a depth z and cross-sectional area for the *i-th* fictitious pile unit, respectively; and E_* is the Young's modulus of the fictitious pile unit and can be expressed as $E_*=E_p-E_s$.

2.3 Extended soil

For the extended soil, $\sigma_z^r(z)$, $\varepsilon_z^r(z)$ and $w_z^r(z)$ represent the vertical stress, vertical strain, and settlement in region $\Pi(z)$ at the position of the *r-th* (r=1,2,…,m) extended soil unit, which can expressed by the superposition principle as follows.

$$\sigma_z^r(z)=\sum_{j=1}^{n}\begin{Bmatrix}\left[P^j(0)+P_*^j(0)\right]\sigma_z^{rj}(z,0)\\ -P_*^j(l_j)\sigma_z^{rj}(z,l_j)-\int_0^{l_j}q^j(\xi)\sigma_z^{rj}(z,\xi)d\xi\end{Bmatrix} + \sum_{k=n+1}^{m}Q^k(0)\sigma_z^{rk}(z,0) \quad (0\le z\le h_r) \tag{4}$$

$$\varepsilon_z^r(z)=\sum_{j=1}^{n}\begin{Bmatrix}\left[P^j(0)+P_*^j(0)\right]\varepsilon_z^{rj}(z,0)\\ -P_*^j(l_j)\varepsilon_z^{rj}(z,l_j)-\int_0^{l_j}q^j(\xi)\varepsilon_z^{rj}(z,\xi)d\xi\end{Bmatrix} + \sum_{k=n+1}^{m}Q^k(0)\varepsilon_z^{rk}(z,0) \quad (0\le z\le h_r) \tag{5}$$

$$w_z^r(z)=\sum_{j=1}^{n}\begin{Bmatrix}\left[P^j(0)+P_*^j(0)\right]w_z^{rj}(z,0)\\ -P_*^j(l_j)w_z^{rj}(z,l_j)-\int_0^{l_j}q^j(\xi)w_z^{rj}(z,\xi)d\xi\end{Bmatrix} + \sum_{k=n+1}^{m}Q^k(0)w_z^{rk}(z,0) \quad (0\le z\le h_r) \tag{6}$$

where $\sigma_z^{rj}(z,\xi)$, $\varepsilon_z^{rj}(z,\xi)$, and $w_z^{rj}(z,\xi)$ are the influence coefficient of the average vertical stress, vertical strain, and settlement of the extended soil in region $\Pi(z)$ at the *r-th* unit due to the uniform distribution and unit load in region $\Pi(\xi)$ at the *j-th* fictitious pile unit, respectively.

Calculations of the stresses and displacements in layered elastic systems are important in engineering analyses and designs. Solutions to the stresses and settlements in two horizontal layered systems were derived by Burmister (1945). The pile-soil-raft interactions were determined through the modified Mindlin solutions (Mindlin 1936) based on the Steinbrenner approximation by Kitiyodom and Matsumoto (2003). The stresses and displacements within an elastic layer as underlain by a rough rigid base were also evaluated numerically by Poulos (1967), which showed that the discrepancy is not significant except for shallow layers with μ=0.5 compared with a semi-infinite mass. Butterfield and Banerjee (1971a, b) found negligible effects on the load sharing and load displacement behavior of pile groups without considering the radial displacement compatibility at the pile-soil interface for compressible piles. More importantly, the integral of Bessel functions should be considered for all analytic solutions of stresses and displacements in horizontal layered elastic systems, which is not easy for practical engineering designs. For inclined bedrock, there is no existing analytic solution for stresses and settlement. Therefore, the vertical stress and settlement influence coefficients are derived by integrating Mindlin's solutions directly for simplification. Then, the vertical strain can be attained from the differential settlement influence solution.

A finite jump exists at $z=\xi$ for $\sigma_z^{ii}(z,\xi)$ and $\varepsilon_z^{ii}(z,\xi)$. The $\sigma_z^{rj}(z,\xi)$, $\varepsilon_z^{rj}(z,\xi)$, and $w_z^{rj}(z,\xi)$ can be derived by combining Eqs. (2) and (4)-(6) as follows.

$$\begin{aligned}\sigma_z^r(z)=&P_*^i(z)\left[\sigma_z^{ii}(z,z^-)-\sigma_z^{ii}(z,z^+)\right]\\ &-\sum_{j=1}^{n}\int_0^{l_j}P_*^j(\xi)\frac{\partial\sigma_z^{rj}(z,\xi)}{\partial\xi}d\xi+\sum_{j=1}^{n}P^j(0)\sigma_z^{rj}(z,0)\\ &+\sum_{k=n+1}^{m}Q^k(0)\sigma_z^{rk}(z,0)\end{aligned} \tag{7}$$

$$\begin{aligned}\varepsilon_z^r(z)=&P_*^i(z)\left[\varepsilon_z^{ii}(z,z^-)-\varepsilon_z^{ii}(z,z^+)\right]\\ &-\sum_{j=1}^{n}\int_0^{l_j}P_*^j(\xi)\frac{\partial\varepsilon_z^{rj}(z,\xi)}{\partial\xi}d\xi+\sum_{j=1}^{n}P^j(0)\varepsilon_z^{rj}(z,0)\\ &+\sum_{k=n+1}^{m}Q^k(0)\varepsilon_z^{rk}(z,0)\end{aligned} \tag{8}$$

$$\begin{aligned}w_s^r(z)=&-\sum_{j=1}^{n}\int_0^{l_j}P_*^j(\xi)\frac{\partial w_z^{rj}(z,\xi)}{\partial\xi}d\xi+\sum_{j=1}^{n}P^j(0)w_z^{rj}(z,0)\\ &+\sum_{k=n+1}^{m}Q^k(0)w_z^{rk}(z,0)\end{aligned} \tag{9}$$

where $\varepsilon_z^{ii}(z,z^+)-\varepsilon_z^{ii}(z,z^-)=\dfrac{(2\mu-1)(1+\mu)}{E_sA(1-\mu)}$ and $\sigma_z^{ii}(z,z^+)-\sigma_z^{ii}(z,z^-)=-1/A$ are obtained from the generalized Hook's law and equilibrium equation, respectively.

2.4 Governing integral equations

The governing equation is established by imposing the strain average compatibility at corresponding depths between the fictitious piles and extended soil.

$$\begin{aligned}&\left[-\frac{1}{E_*}-\frac{(1-2\mu)(1+\mu)}{E_s(1-\mu)}\right]P_*^i(z)+A\sum_{j=1}^{n}\int_0^{l_j}P_*^i(\xi)\frac{\partial\varepsilon_z^{ij}(z,\xi)}{\partial\xi}d\xi\\ &=A\left(\sum_{j=1}^{n}P^j(0)\varepsilon_z^{ij}(z,0)+\sum_{k=n+1}^{m}Q^k(0)\varepsilon_z^{ik}(z,0)\right)\end{aligned} \tag{10}$$

This is known as the Fredholm integral equation of the second kind, where the axial forces of the fictitious pile are the unknown parameters. Once the vertical load of all unit tops is known, a definite solution can be obtained and the load transfer mechanism and settlement characteristics for

the pile group without a raft or pile group with an absolute flexibility cap can be analyzed directly.

2.5 Analytical solution

Once the axial forces of all fictitious piles $P_*^i(z)$ (i=1,2,…,n) have been calculated, the real axial force of all units $P^r(z)$ (r=1,2,…,m) can be expressed as the difference between $P_*^i(z)$ and $\sigma_z^r(z)A$

$$\begin{aligned} P^r(z) = &-A\sum_{j=1}^{n}\int_0^{l_j} P_*^j(\xi)\frac{\partial\sigma_z^{rj}(z,\xi)}{\partial\xi}d\xi \\ &+A\sum_{j=1}^{n}P^j(0)\sigma_z^{rj}(z,0)+A\sum_{k=n+1}^{m}Q^k(0)\sigma_z^{rk}(z,0) \end{aligned} \tag{11}$$

The loading of each unit top $P^r(0)$ can be obtained by supposing z=0 in Eq. (11). The settlement of pile units $w_p^j(z)$ are coincident with the extended soil in the corresponding position $w_s^r(z)$, which means that when r=i, we have

$$w_p^j(z)=w_s^r(z) \quad (r=i) \tag{12}$$

Thus, the effect of the underlying inclined bedrock on settlement is now considered. It is reasonable to assume there is no settlement at the bedrock position for each unit, so the real settlement at a finite soil of depth h_r for the *r-th* unit can be written as

$$W^r(z)=w_s^r(z)-w_s^r(h_r) \quad (r=1,2,\ldots,m) \tag{13}$$

The surface settlement of each unit $W^r(0)$ can be written by supposing the z=0 in Eq. (13).

2.6 Numerical solution

For the pile group or PCF with a rigid cap, the vertical load of each unit top is unknown. Thus, the governing Eq. (10) cannot be solved directly, and supplementary equations are needed. For the rigid cap, the average settlement w_{ave} and inclination slope θ of the cap should be compatible with the surface settlement of each unit $W^r(0)$. Then, we have

$$W^r(0)=w_{ave}+\theta\mathbf{\Omega} \quad (r=1,2,\ldots,m) \tag{14}$$

where $\mathbf{\Omega}$ is the location matrix of each element and can be readily obtained from the coordinate system.

Enforcing static equilibrium conditions between the pile-soil-cap system indicates that the total load of all unit tops should be equal to the vertical load N_0 as

$$\begin{aligned} N_0=&\sum_{i=1}^{n}P_p^i(0)+\sum_{k=n+1}^{m}Q^k(0) \\ &(i=1,2,\ldots,n,\ k=n+1,n+2,\ldots,m) \end{aligned} \tag{15}$$

The axial forces of the fictitious pile $P_*^i(z)$ can be solved by combining Eqs. (10), (14), and (15). Then, the axial forces and settlement of each unit along the depth can be obtained.

Solving the governing integral in Eq. (10) is the key step toward a reasonable solution. The methods to solve the Fredholm integral equation of the second kind can be classified into five categories: analytical and semi-analytical methods, kernel approximation methods, projection methods, quadrature algorithms, and Volterra and initial value methods (Golberg 1979). The numerical integration to transform the integration into algebraic equations is a common and relatively simple approach. The main processes are given as follows. Suppose all units are divided into small segments where s_r is the total node number of the r-th unit. Then, the total node number for n pile units is $N_1=\sum_{r=1}^{n}s_r$, for the rest of the m-n soil units is $N_2=\sum_{k=n+1}^{m}s_k$, and for all units is N=N_1+N_2.

Obviously, the small segment length is a vital parameter for the finally analysis results. It is well known that the numerical solution for Fredholm integral equation of the second kind is relative stable (Golberg 1979). Liang (2009, 2014) has proposed that computational efficiency and accuracy can meet requirements when the ratio of small segment length to pile diameter less than 0.5. Therefore, the small segment length is chosen 0.2 times pile diameter in this paper.

The z_α (α=1,2,...,s_r) denotes the depth of the selected nodes in the r-th unit. Thus, Eq. (10) can be rewritten as

$$\begin{aligned} &\left[-\frac{1}{E_*}-\frac{(1-2\mu)(1+\mu)}{E_s(1-\mu)}\right]P_*^i(z_\chi)+A\sum_{j=1}^{n}\sum_{\alpha=1}^{s_j}P_*^j(z_\alpha)\frac{\partial\varepsilon_z^{ij}(z_\chi,z_\alpha)}{\partial z_\alpha} \\ &=A\left(\sum_{j=1}^{n}P^j(0)\varepsilon_z^{ij}(z_\chi,0)+\sum_{k=n+1}^{m}Q^k(0)\varepsilon_z^{ik}(z_\chi,0)\right) \end{aligned} \tag{16}$$

The meaning of index χ is the same as index α. Eq. (16) shows algebraic equations and should be transformed into an expanded algebraic equation for programming requirements.

The scalar $L=\sum_{r=1}^{m}h_r$ is defined to represent the sum of all element depths, and the range of the parameters z_α and z_χ are expanded to [0,L]. The z and ξ denote the serial number in the corresponding matrix. The vector $\left[\overrightarrow{\mathbf{P_V}}\right]_{N_1\times1}$ is formed from the axial force of all fictitious pile units. When $\sum_{j=1}^{i-1}h_j\le z_\alpha\le\sum_{j=1}^{i}h_j$, we have

$$\overrightarrow{\mathbf{P_V}}(z,1)=P_*^i\left(z_\alpha-\sum_{j=1}^{i-1}h_j\right) \quad (i=1,2,\ldots,n) \tag{17}$$

The axial force of the fictitious pile units between the pile bottom and bedrock should be set to 0 as no fictitious pile exists. The vector $\left[\overrightarrow{\mathbf{ARN}}\right]_{N\times1}$ represents the real axial force of all the units. When $\sum_{j=1}^{r-1}h_j\le z_\alpha\le\sum_{j=1}^{r}h_j$, we have

$$\overrightarrow{\mathbf{ARN}}(z,1)=P_p^r\left(z_\alpha-\sum_{j=1}^{r-1}h_j\right) \quad (r=1,2,\ldots,m) \tag{18}$$

The real axial force atop each unit, $\left[\overrightarrow{\mathbf{ARN0}}\right]_{m\times 1}$, can be obtained from the transformation matrix $\mathbf{T1}$ and vector $\left[\overrightarrow{\mathbf{ARN}}\right]_{N\times 1}$ as

$$\overrightarrow{\mathbf{ARN0}}=\mathbf{T1}\cdot\overrightarrow{\mathbf{ARN}} \tag{19}$$

The transformation matrix $\mathbf{T1}$ can be achieved in matlab program as follows. As mentioned above, the total node number for m units are N, and the node number of the r-th unit is s_r, and $N=\sum_{r=1}^{m}s_r$. Therefore, the vector $\left[\overrightarrow{\mathbf{ARN}}\right]_{N\times 1}$ can be rearranged into cell array with $m\times 1$ dimension. Then the r-th content of cell array is about the r-th unit axial force, and the axial force of each unit head can be obtained by extracting the first value.

The vector $\left[\overrightarrow{\mathbf{ARW}}\right]_{N\times 1}$ denotes the settlement of all units. When $\sum_{j=1}^{r-1}h_j\le z_\alpha\le\sum_{j=1}^{r}h_j$, we have

$$\overrightarrow{\mathbf{ARW}}(z,1)=w_s^r\left(z_\alpha-\sum_{j=1}^{r-1}h_j\right)\quad(r=1,2,\ldots,m) \tag{20}$$

The settlement atop each unit considering the influence of the inclined bedrock $\left[\overrightarrow{\mathbf{ARW0}}\right]_{m\times 1}$ can be obtained using the transformation matrix $\mathbf{T2}$ and vector $\left[\overrightarrow{\mathbf{ARW}}\right]_{N\times 1}$

$$\overrightarrow{\mathbf{ARW0}}=\mathbf{T2}\cdot\overrightarrow{\mathbf{ARW}} \tag{21}$$

The formulation of transformation matrix $\mathbf{T2}$ is the same with $\mathbf{T1}$.

For a given unit load atop each unit, the response of the vertical strain for n units as occupied by piles can be expressed as the matrix $\left[\mathbf{EZ0A2P}\right]_{N_1\times m}$ and is calculated as follows. When $\sum_{j=1}^{r-1}h_j\le z_\alpha\le\sum_{j=1}^{r}h_j$, we have

$$\mathbf{EZ0A2P}(z,r)=\varepsilon_z^{ir}\left(z_\alpha-\sum_{j=1}^{i-1}h_j,0\right)\quad(i=1,2,\ldots,n,\ r=1,2,\ldots,m) \tag{22}$$

The unit load atop each unit leads to vertical stresses for all units, which is expressed as the vertical stress matrix $\left[\mathbf{SZ0A2A}\right]_{N\times m}$. When $\sum_{j=1}^{r-1}h_j\le z_\alpha\le\sum_{j=1}^{r}h_j$, we have

$$\mathbf{SZ0A2A}(z,r)=\sigma_z^{tr}\left(z_\alpha-\sum_{j=1}^{r-1}h_j,0\right)\quad(r=1,2,\ldots,m,\ t=1,2,\ldots,m) \tag{23}$$

The unit load atop each unit will lead to settlement for all units, which is expressed as the settlement matrix $\left[\mathbf{WZ0A2A}\right]_{N\times m}$. When $\sum_{j=1}^{r-1}h_j\le z_\alpha\le\sum_{j=1}^{r}h_j$, we have

$$\mathbf{WZ0A2A}(z,r)=w_z^{tr}\left(z_\alpha-\sum_{j=1}^{r-1}h_j,0\right)\quad(r=1,2,\ldots,m,\ t=1,2,\ldots,m) \tag{24}$$

The matrix $\left[\mathbf{KEP2P}\right]_{N_1\times N_1}$ denotes the vertical strain influence matrix between n pile units. When $\sum_{j=1}^{r-1}h_j\le z_\alpha\le\sum_{j=1}^{r}h_j$ and $\sum_{j=1}^{\psi-1}h_j\le z_\chi\le\sum_{j=1}^{\psi}h_j$, we have

$$\mathbf{KEP2P}(z,\xi)=K_\varepsilon^{i\psi}\left(z_\alpha-\sum_{j=1}^{i-1}h_j,z_\chi-\sum_{j=1}^{\psi-1}h_j\right)\quad(i=1,2,\ldots,n,\ \psi=1,2,\ldots,n) \tag{25}$$

The unit load of n pile units leads to vertical stresses for all units, which is expressed as the vertical stress matrix $\left[\mathbf{KSP2A}\right]_{N\times N_1}$. When $\sum_{j=1}^{i-1}h_j\le z_\alpha\le\sum_{j=1}^{i}h_j$ and $\sum_{j=1}^{r-1}h_j\le z_\chi\le\sum_{j=1}^{r}h_j$, we have

$$\mathbf{KSP2A}(z,r)=\frac{\partial\sigma_z^{ri}\left(z_\alpha-\sum_{j=1}^{i-1}h_j,z_\chi-\sum_{j=1}^{r-1}h_j\right)}{\partial z_\chi}\quad(i=1,2,\ldots,n;\ r=1,2,\ldots,m) \tag{26}$$

The unit load of n units occupied by piles leads to settlement for all units, which is expressed as the settlement matrix $\left[\mathbf{KWP2A}\right]_{N\times N_1}$. When $\sum_{j=1}^{i-1}h_j\le z_\alpha\le\sum_{j=1}^{i}h_j$ and $\sum_{j=1}^{r-1}h_j\le z_\chi\le\sum_{j=1}^{r}h_j$, we have

$$\mathbf{KWP2A}(z,r)=\frac{\partial w_z^{ri}\left(z_\alpha-\sum_{j=1}^{i-1}h_j,z_\chi-\sum_{j=1}^{r-1}h_j\right)}{\partial z_\chi}\quad(i=1,2,\ldots,n;\ r=1,2,\ldots,m) \tag{27}$$

Then, the matrix notation for the algebraic equations can be expressed as

$$\begin{bmatrix}\alpha\cdot\mathbf{I}-\boldsymbol{\lambda}\cdot\mathbf{KEP2P} & \mathbf{EZ0A2P} & \mathbf{0} & \mathbf{0} & \mathbf{0}\\ -\mathbf{KSP2A} & \mathbf{SZ0A2A} & -\mathbf{I} & \mathbf{0} & \mathbf{0}\\ -\mathbf{KWP2A} & \mathbf{WZ0A2A} & \mathbf{0} & -\mathbf{I} & \mathbf{0}\\ \mathbf{0} & \mathbf{I} & \mathbf{0} & \mathbf{0} & \mathbf{0}\\ \mathbf{0} & \boldsymbol{\delta} & \mathbf{0} & \mathbf{T} & -\mathbf{I}\end{bmatrix}\begin{Bmatrix}\overrightarrow{\mathbf{P_V}}\\ \overrightarrow{\mathbf{ARN0}}\\ \overrightarrow{\mathbf{ARN}}\\ \overrightarrow{\mathbf{ARW}}\\ \overrightarrow{\mathbf{WC}}\end{Bmatrix}=\begin{Bmatrix}\vec{\mathbf{0}}\\ \vec{\mathbf{0}}\\ \vec{\mathbf{0}}\\ N_0\\ \vec{\mathbf{0}}\end{Bmatrix} \tag{28}$$

Eq. (28) is a definite solution equation, as mentioned earlier; however, the dimensions of the equation to be solved may be unacceptable for large PCFs or too many divided segments. This is a sparse matrix based on its coefficients, which leads to a large condition number through program checking.

Therefore, An iterative procedure is proposed to solve this definite problem as the initial values of $P^i(0)$ and $Q^k(0)$ (i=1,2,…,n, k=n+1,n+2,…,m) cannot be known, the basic processes is given in Fig. 3 and briefly introduced as

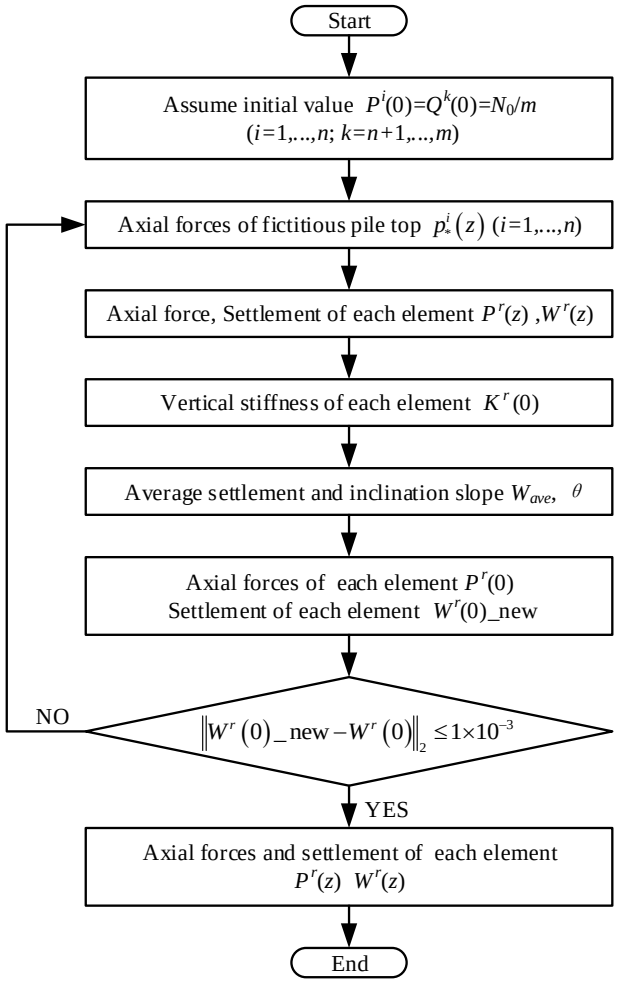

Fig. 3 Solving algorithm based on an iterative process

follows. The first step is to assume the initial load values of each element $P^i(0)=Q^k(0)=N_0/m$ at z=0, the assumption can satisfy the vertical load equilibrium condition. Then, the axial forces of each fictitious pile $P_*^{'}(z)$ can be determined by Eq. (10). The real axial force and settlement of each element $P^r(z)$ and $P^r(z)$ can be obtained from Eq. (11) and (13). Therefore, the vertical stiffness of atop each element $K^r(0)=P^r(0)/W^r(0)$ can be achieved easily. The average settlement and inclination slope of raft W_{ave} and θ can be calculated by establishing the vertical equilibrium equation of raft by the given load condition N_0. Furthermore, the settlement of each element can be obtained again from Eq. (14), and denoted by $W^r(0)$_new, If the cumulative difference between $W^r(0)$_new and $W^r(0)$ cannot be ignored, for instance, $\sum_{r=1}^{m}\|W^r(0)\_new-W^r(0)\|_2 > 1\times10^{-3}$, the real axial force of each element $P^r(0)$ can be recalculated by $P^r(0)=K^r(0)\cdot W^r(0)$ and back to the first step by renewing the initial load values of each element $P^r(0)$, until the $\sum_{r=1}^{m}\|W^r(0)\_new-W^r(0)\|_2 > 1\times10^{-3}$. Finally, we can obtain the axial forces and settlement along depth of each element $P^r(z)$ and $W^r(z)$.

3. Verification of proposed method

To the author's knowledge, there is no theoretical research considering the settlement of dissimilar pile groups located over inclined bedrock. To validate the accuracy of the proposed method, two field load tests of a single pile are performed by considering the enforcement and shielding effect of neighboring piles. A numerical simulation case is also considered.

3.1 Single pile load test

A shallow buried anchorage foundation was proposed for Honghe bridge in Yunnan province. The bottom of the foundation is 48 × 62 m and the average embedded depth is approximately 15 m. The back-toe area of the foundation is located on the moderately weathered slate, and the front toe area is on the strongly weathered slate, as shown in Fig. 4.

The rigid PCF is set at the strongly weathered slate area to reduce the differential settlement and increase the anti-overturning stability of the anchorage foundation. The rigid piles are arranged in a rectangular layout with a diameter of 1.2 m, pile spacing of 4.5 m, and pile length that varies with the embedded depth of the inclined strongly weathered slate. The elastic parameters of the strongly weathered slate and rigid piles are given with E_p and E_s as 30 GPa and 300 MPa and μ being equal to 0.25. The load tests for a single pile were performed at two locations on the project site, as

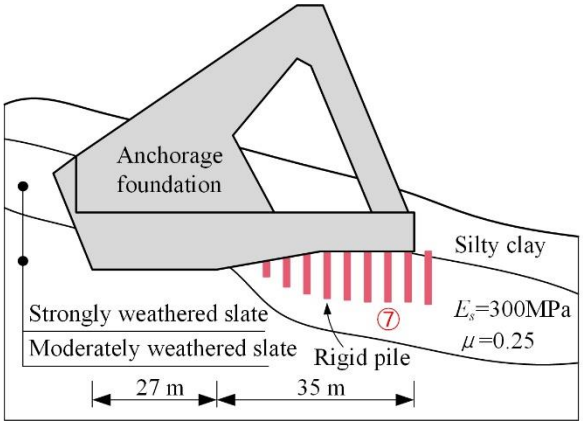

Fig. 4 Schematic diagram of the PCF

Fig. 5 Field load test of a single pile

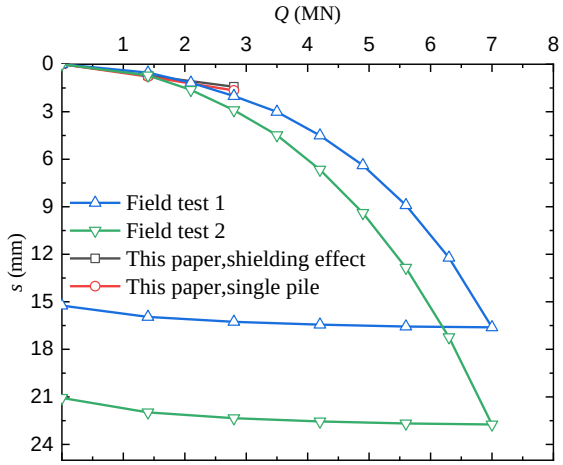

Fig. 6 Load settlement curves of the field tests and theoretical method

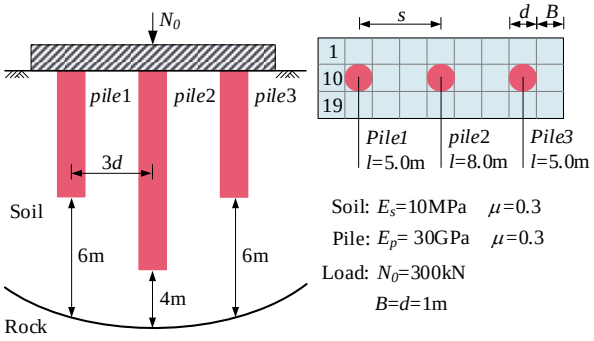

Fig. 7 PCF configuration and parameters

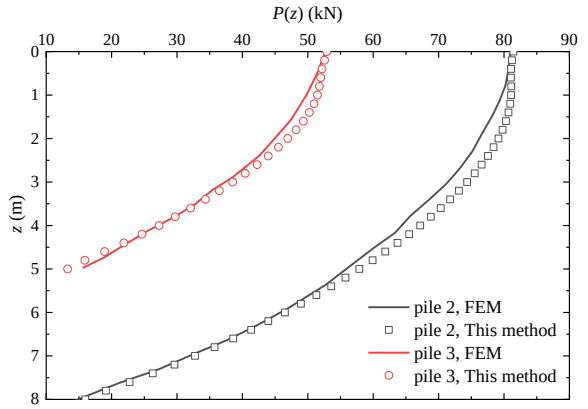

(a) Axial force distribution curve

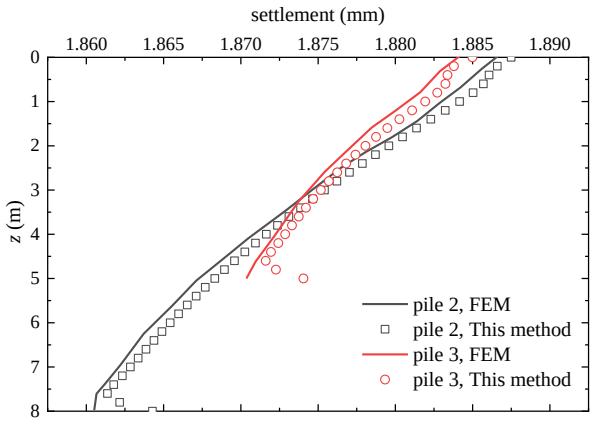

(b) settlement distribution curve

Fig. 8 Comparison of calculated solutions for PCF

indicated by the 7-*th* row in Fig. 4. The pile length and embedded depth of the moderately weathered slate for the 7-*th* row are located at approximately 9.4 and 15 m, respectively.

The neighboring piles exist when loading a single pile; therefore, it is necessary to consider the enforcement and shielding effect of neighboring piles. The pile was loaded using a hydraulic jack attached to the pile and a reaction frame, as shown in Fig. 5.

The *Q-s* curves of the load test are presented as comparisons with the proposed method in Fig. 6. The curves from the field load tests are similar to the theoretical solutions at the initial stage. As the loading increases, the curvature of the *Q-s* curves increases gradually as the plastic settlement emerges. Therefore, a significant difference may exist between the proposed method and field load tests as the proposed method cannot consider plastic deformation. Comparing the theoretical solutions indicates the enforcement and shielding effect of neighborhood piles can have limited improvements in the pile stiffness due to the large pile spacing.

3.2 Vertical loaded dissimilar PCF

A comparison of the 3×1 PCF calculated using the proposed method and FEM is performed to further verify the feasibility of the proposed method. The 3×1 PCF having dissimilar pile length and rigid cap over inclined bedrock is modeled, and the input parameters are illustrated in Fig. 7. The calculated results of the proposed method and the simplified analytical method are compared based on the axial force and settlement distribution along pile shaft for pile 2 and pile 3, as shown in Fig. 8. Fig. 8 shows that the results obtained from the proposed method reasonably match FEM solutions. Therefore, the proposed method is considered reliable.

4. Result and discussion

4.1 Solutions for 3-PCF

A 3-pile PCF with a rigid cap over inclined bedrock is examined, as shown in Fig. 9. The settlement characteristics, load transfer behavior, and load sharing ratio of the PCF are evaluated with the given parameters. The soil and pile parameters are shown in Fig. 9. To cover the range of pile properties for major practical interests, E_p=30 GPa is considered for rigidly reinforced concrete piles, and E_p=200 MPa is considered for flexible piles with s=3d and B/d=1. The inclined angle of the bedrock α is set to 30°, the length (l) of pile 2 is 5.8 m, and the distance Δ between each pile bottom and the inclined bedrock is set to be equal at Δ=1 m. Then, the length of piles 1 and 3 can be determined.

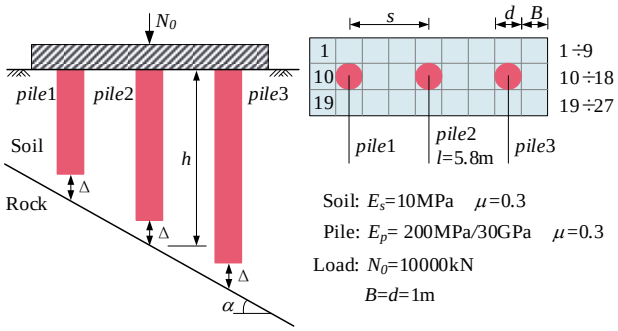

Fig. 9 3-PCF embedded over inclined bedrock

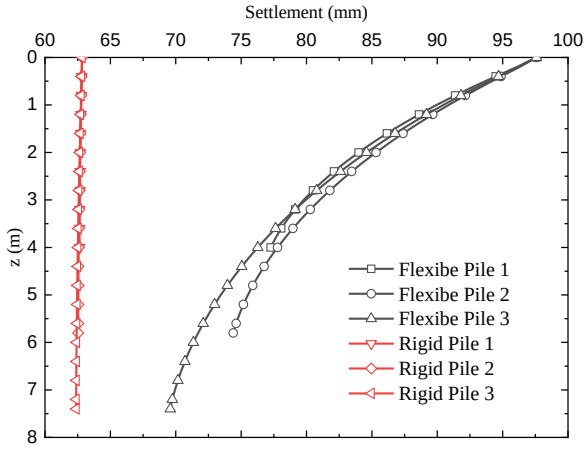

Fig. 10 Settlement distribution curves

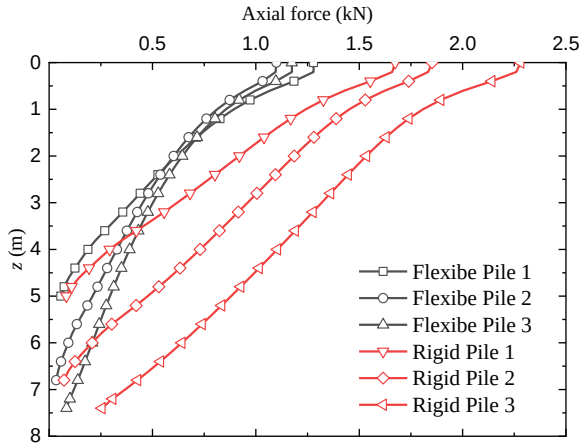

Fig. 11 Axial force distribution curves

The settlement and axial force distributions along the pile length are shown in Figs. 10 and 11, respectively. There is a strong effect from the pile-soil stiffness ratio k (k=E_p/E_s) on the PCF behavior. For the rigid PCF, pile compression is negligible and the settlement is an approximately 35% reduction. The axial force for individual piles increases markedly compared with the flexible pile.

4.2 Influence of distance between pile bottom and inclined bedrock

A 3-pile PCF with a rigid cap over inclined bedrock is taken as the first parameter analysis example. The model

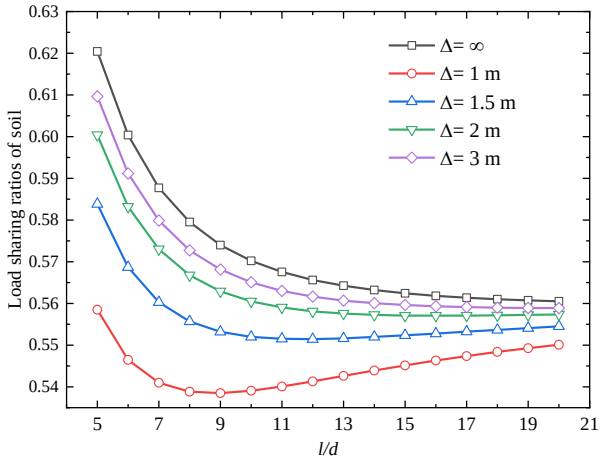

Fig. 12 Load sharing ratios of soil for flexible piles (k=30)

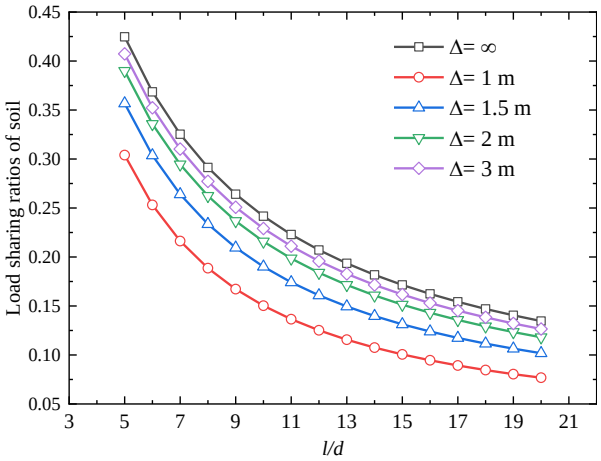

Fig. 13 Load sharing ratios of soil for rigid piles (k=3000)

and basic parameters (except Δ and l) are consistent with Fig. 9. Figs. 12 and 13 depict the effects of Δ on the load sharing ratios of the soil considering different l/d and k. The range of l/d is from 5-20, and k values of 30 and 3000 are selected as the comparison cases. The k values are chosen to cover flexible and rigid piles in practice. The vertical stiffness of piles increases due to the greater l/d; therefore, the load sharing ratio of the soil decreases with l/d for both flexible and rigid piles. The values of the load sharing ratio of the soil for flexible piles are significantly larger than for rigid piles, as shown in Figs. 12 and 13. The load sharing ratio of soil with a semi-infinite medium is always greater than the finite depth conditions as the existence of bedrock can contribute to strengthened pile-soil load sharing ratios. There is no obvious impact when Δ is larger than 3 m due to the limited influence depth of the pile bottom stress.

Figs. 14 and 15 show the effects of Δ on the non-dimensional vertical stiffness N_0/wdE_s with different l/d and k, where w is the average settlement of the composite foundation. For a semi-infinite medium, the vertical stiffness increases with l/d for both flexible and rigid piles. Meanwhile, comparing the finite depth and semi-infinite medium conditions shows there is a noticeable increase in the vertical stiffness due to the bedrock, which is consistent with Poulos (1967). Fig. 14 shows that the vertical stiffness

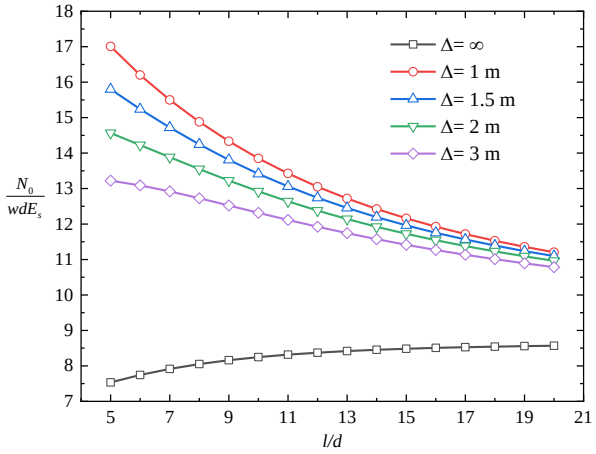

Fig. 14 Total stiffness of flexible PCFs (k=30)

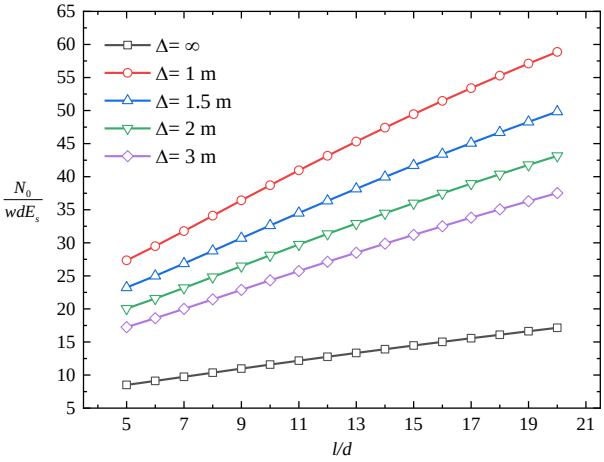

Fig. 15 Total stiffness of rigid PCFs (k=3000)

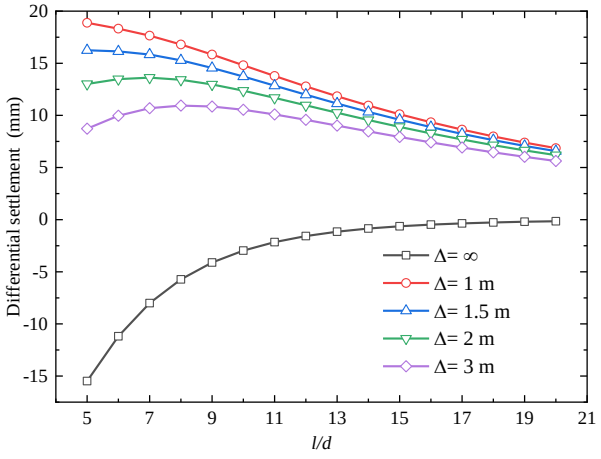

Fig. 16 Differential settlement of flexible PCF (k=30)

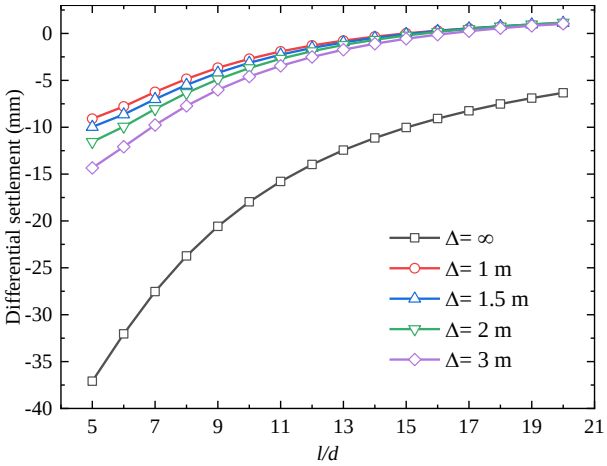

Fig. 17 Differential settlement of rigid PCF (k=3000)

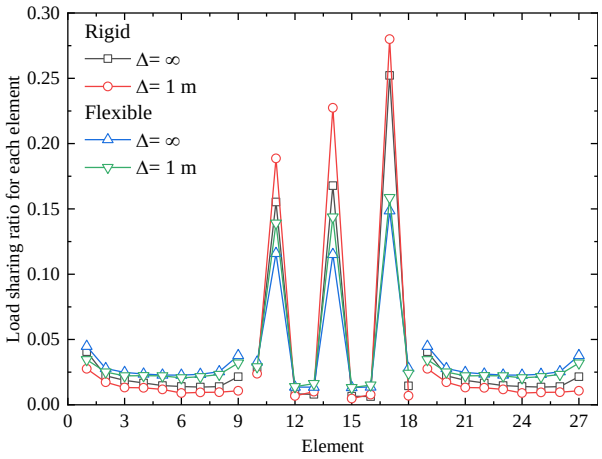

Fig. 18 Load sharing ratios of each element for l/d=5

of the system decreases with l/d and is less affected when l/d >15 for all finite depth conditions. This is because the settlement and load transfer tend to be negligible beyond the effective pile length for flexible piles. Fig. 15 shows that the vertical stiffness increases linearly with l/d and changes significantly for different Δ.

The differential settlement of the foundations can be observed to describe the impact of the inclined bedrock, as shown in Figs. 16 and 17. For a semi-infinite medium, the negative sign of the differential foundation settlements is specified as counterclockwise, which means the settlement of pile 1 is larger than pile 3 as it is shorter. For the flexible PCF, Fig. 16 presents the positive differential settlement for the foundation, which decrease with l/d for different Δ. Thus, the vertical stiffness of pile 3 is smaller than pile 1 even though it is longer due to the existence of the inclined bedrock. For the rigid PCF, the trends of differential settlements over Δ are consistent with the semi-infinite medium, as illustrated in Fig. 17. The differential settlement is much smaller, which demonstrates that the vertical stiffness of each element tends to be uniform due to the effect of the inclined bedrock.

The PCF element number is indicated in Fig. 9. To further investigate the pile-soil load sharing ratio for each element, two conditions of l/d=5 and 20 are calculated, as shown in Figs. 18 and 19. It is noted that the load sharing ratio of corner elements is greater than side elements and that the side elements are larger than center elements due to the pile-soil-cap interactions under all conditions, which agrees well with the available solutions from Randolph and Wroth (1979). In particular, the increased pile-soil load sharing ratio is observed for Δ=1 m compared with the semi-infinite medium. Fig. 18 illustrates the load sharing

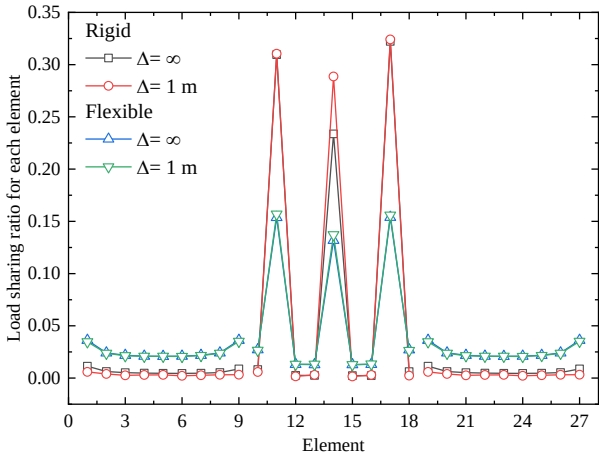

Fig. 19 Load sharing ratios of each element for *l*/*d*=20

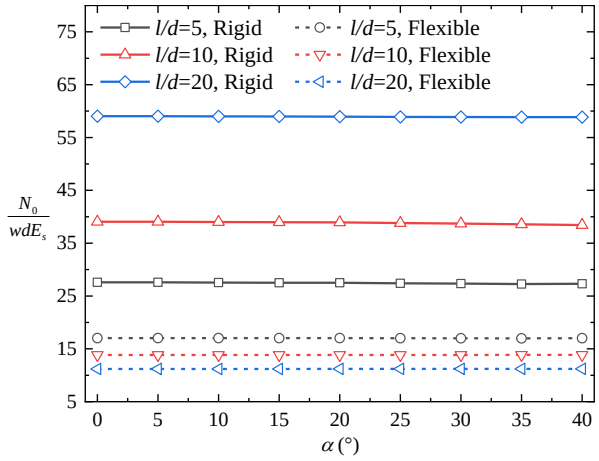

Fig. 20 Total stiffness of PCF

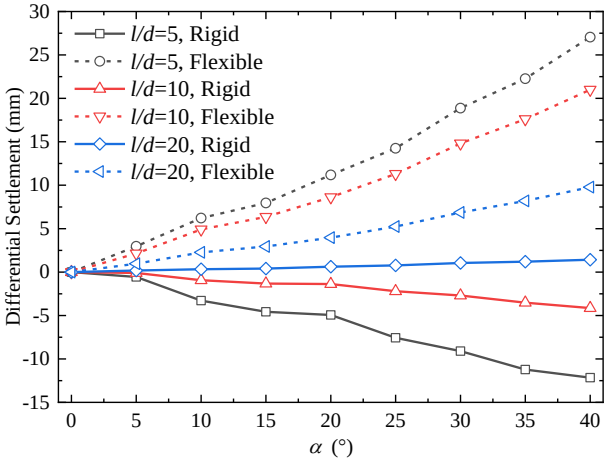

Fig. 21 Differential settlement of PCF

ratio for each element with *l*/*d*=5. The average pile-soil load sharing ratio for rigid piles is approximately 5.69 and 7.25 considering $\Delta=\infty$ and Δ=1 m, respectively, and is about 3.48 and 4.14 for flexible piles. The vertical stiffness of the pile elements increases with *l*/*d*; therefore, the average pile-soil load sharing ratio for rigid piles is about 9.73 and 10.67 considering $\Delta=\infty$ and Δ=1 m, respectively, and is about 4.12 and 4.23 for flexible piles, as shown in Fig. 19.

4.3 Influence of bedrock inclined angle

The 3-pile PCF model proposed in Fig. 9 is considered to further investigate the effects of the bedrock inclined angle on the PCF. The total length of 3 piles is set as a constant parameter and Δ=1 m is maintained as the inclined angle changes from 0° to 40°. Fig. 20 illustrates the effect of the inclined bedrock on the non-dimensional vertical stiffness N_0/wdE_s of the foundation. The vertical stiffness of the foundation is influenced slightly by the inclined angle as the total length of the 3 piles is unchanged for each condition, while the length and vertical stiffness of the piles have a significant impact. Considering the rigid pile, the vertical stiffness N_0/wdE_s for *l*/*d*=10 and 20 is approximately 42% and 114% higher than that for *l*/*d*=5, respectively. It is concluded that Δ strengthens the vertical stiffness for each condition of *l*/*d* due to the strong load transfer capacity. In contrast, the flexible pile reduces the vertical stiffness N_0/wdE_s for *l*/*d*=10 and 20 by approximately 66% and 81% compared with *l*/*d*=5, respectively. This indicates that Δ plays an important role in strengthening the vertical stiffness for smaller *l*/*d* conditions due to the weaker load transfer capacity.

Fig. 21 shows that the differential settlement in the foundation increases linearly with the inclined angle for all conditions. The opposite rotation direction for the foundation is observed for different stiffness ratios. When there is less (more) settlement for the shorter pile, pile 1 than the longer pile, pile 3, the sign of the differential settlement is positive (negative). The positive sign in the differential settlement for all flexible pile conditions is observed with a larger absolute value compared to rigid piles in the corresponding case. This means that Δ plays a key role in improving the vertical stiffness of pile 1, even though it is shorter than pile 3. The influence of the inclined angle on the differential settlement decreases gradually as the difference in the head stiffness for each pile tends to be identical with an increased *l*/*d*.

Figs. 22-25 show the load sharing ratio of typical elements, such as corner elements (element 1, element 9), side element (element 5), and pile elements (element 11, 14, and 17) under different *l*/*d* and pile-soil stiffness ratios. The results indicate that the varied bedrock inclined angle has a minor influence on the middle pile (element 14) and side (element 5), while the load sharing ratios of the piles are much larger than the soil. The load sharing ratios of the middle pile (element 14) are lower than the side pile (elements 11 and 19) for *l*/*d*=20 and 5 when α is less than 15 due to the enforcement and shielding effect of neighboring elements. The same trend for soil elements is also observed.

For *l*/*d*=5, the load sharing ratios of pile element 11 and soil element 1 increase with the inclined angle, while pile element 17 and soil element 9 vary with an opposite pattern. These results were also obtained by Roh and Kim (2019). It is noted that the effect of the inclined angle on the load sharing ratio gradually decreases with *l*/*d*, which is consistent with the results from Fig. 21.

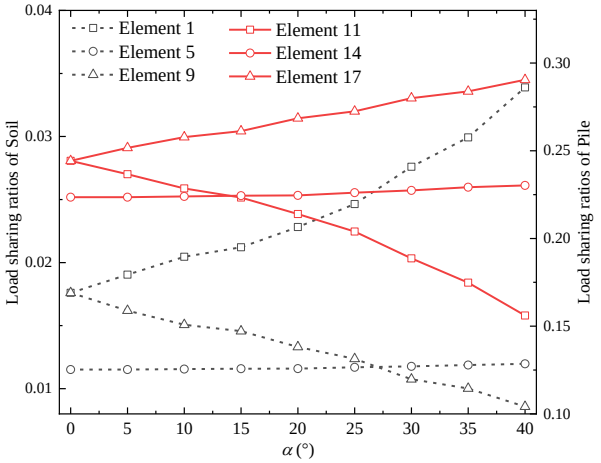

Fig. 22 Load sharing ratios of typical elements for *l*/*d*=5 and rigid piles

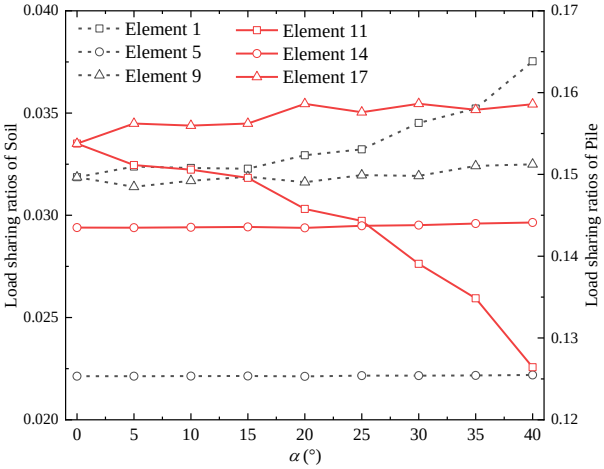

Fig. 23 Load sharing ratios of typical elements for *l*/*d*=5 and flexible piles

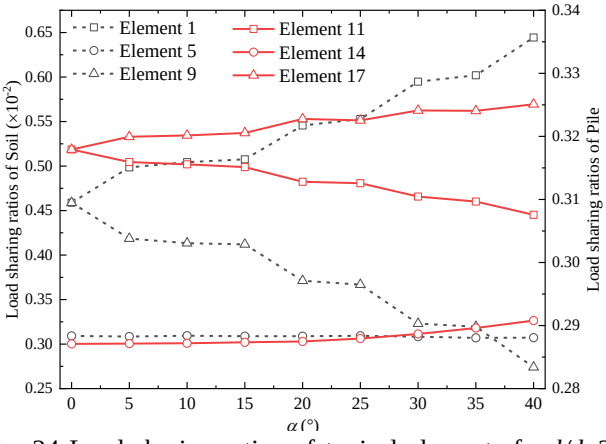

Fig. 24 Load sharing ratios of typical elements for *l*/*d*=20 and rigid piles

5. Conclusions

This paper developed a simplified analytical method and investigated the effects of embedded inclined bedrock on PCFs having dissimilar pile lengths. The analytical model, governing equations, and iterative algorithm for an *n*-pile

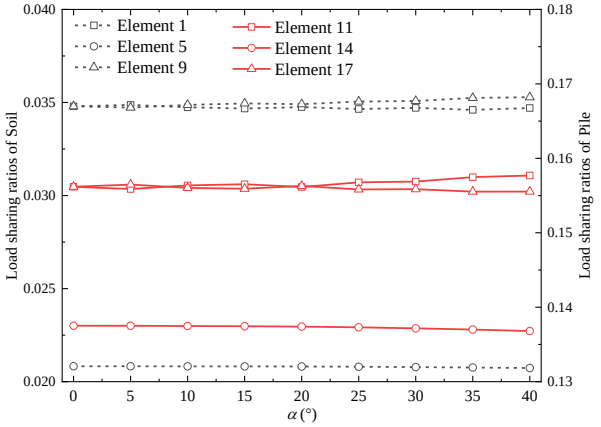

Fig. 25 Load sharing ratios of typical elements for *l*/*d*=20 and flexible piles

PCF are presented. Two field load tests for a single pile and FEM analysis of 3-pile dissimilar PCF are induced and validated with the theoretical results. Then, a typical 3-pile PCF having dissimilar pile lengths located above inclined bedrock is taken as an example. The settlement characteristics and load transfer behaviors are obtained, and the effects of the embedded depth and incline angle of the bedrock are also determined. The principal findings are summarized as follows:

(1) The developed theoretical model efficiently predicts the single pile and 3-pile PCF located over bedrock. A significant difference is observed in the settlement and load transfer behaviors for the 3-pile PCF under different pile-soil stiffness ratios.

(2) The embedded depth of the inclined bedrock significantly impacts the pile-soil load sharing ratios and non-dimensional vertical stiffness N_0/wdE_s for different *l*/*d*. These both increase for smaller Δ. More significant effects are found for the rigid PCF.

(3) The differential settlement and pile-soil load sharing ratios are influenced by the inclined angle of bedrock for both rigid and flexible piles, while only slight effects are shown for *l*/*d*=20.

Acknowledgements

This research was supported by the National Natural Science Foundation of China (52178317, 52078128), the Technological Research Program of Chongqing Municipal Education Commission (KJQN202101236), the Natural Science Foundation of the Jiangsu Higher Education Institutions of China (22KJB560034). The authors are grateful for their support.

References

Abdrabbo, F.M. and El-wakil, A.Z. (2015), "Behavior of pile group incorporating dissimilar pile embedded into sand", *Alexandria Eng. J.*, **54**(2), 175-182. https://doi.org/10.1016/j.aej.2014.11.001.

Bai, X.H., He, W.B., Jia, J.G. and Han, Y.S. (2006), "Experimental

study on the interaction mechanism of cap-pile group-soil", *Mar. Georesour. Geotec.*, **24**(3), 173-182. https://doi.org/10.1080/10641190600788254.

Banerjee, P.K. and Davies, T.G. (1978), "The behaviour of axially and laterally loaded single piles embedded in nonhomogeneous soils", *Geotechnique*, **28**(3), 309-326. https://doi.org/10.1680/geot.1978.28.3.309.

Burmister, D.M. (1945), "The general theory of stresses and displacements in layered systems. I", *J. Appl. Phys.*, **16**(2), 89-94. https://doi.org/10.1063/1.1707558.

Butterfield, R. and Banerjee, P.K. (1971), "The elastic analysis of compressible piles and pile groups", *Geotechnique*, **21**, 43-60. https://doi.org/10.1680/geot.1971.21.1.43.

Butterfield, R. and Banerjee, P.K. (1971), "The problem of pile group-pile cap interaction", *Geotechnique*, **21**(2), 135-142. https://doi.org/10.1680/geot.1971.21.2.135.

Chen, S.L., Song, C.Y. and Chen, L.Z. (2011), "Two-pile interaction factor revisited", *Can. Geotech. J.*, **48**(5), 754-766. https://doi.org/10.1139/t10-095.

Fatolahzadeh, S., Mehdizadeh, R. and Nadi, B. (2020), "Study of the effect of an inclined bedrock on the bearing capacity of shallow foundations", *Iranian J. Sci. Technol. T. Civil Eng.*, **44**(4), 1359-1372. https://doi.org/https://doi.org/10.1007/s40996-020-00418-5.

Golberg, M.A. (1979), *Solution methods for integral equations*.

Han, J. and Jiang, G. (2011), "Influence of inclined bedrock on undrained bearing capacity of shallow strip foundations", *Adv. Geotech. Eng.*, 322-331. https://doi.org/10.1061/41165(397)34.

Hassona, F., Moussa Abu Bakr, A., Hakeem, B.M., *et al*. (2022), "Finite element simulation of piled raft capacity under different loading conditions", *J. Adv. Eng. Trends*, **42**(1), 141-155. https://doi.org/10.21608/jaet.2021.70440.1106.

Huang, M.S., Liang, F.Y. and Jiang, J. (2011), "A simplified nonlinear analysis method for piled raft foundation in layered soils under vertical loading", *Comput. Geotech.*, **38**(7), 875-882. https://doi.org/10.1016/j.compgeo.2011.06.002.

Kitiyodom, P. and Matsumoto, T. (2002), "A simplified analysis method for piled raft and pile group foundations with batter piles", *Int. J. Numer. Anal. Method. Geomech.*, **26**(13), 1349-1369. https://doi.org/10.1002/nag.248.

Kitiyodom, P. and Matsumoto, T. (2003), "A simplified analysis method for piled raft foundations in non-homogeneous soils", *Int. J. Numer.*, **27**, 85-109. https://doi.org/10.1002/nag.264.

Kodikara, J.K. and Johnston, I.W. (1994), "Analysis of compressible axially loaded piles in rock", *Int. J. Numer. Anal. Method. Geomech.*, **18**(6), 427-437. https://doi.org/https://doi.org/10.1002/nag.1610180606.

Kuwabara, F. (1989), "An elastic analysis for piled raft foundations in a homogeneous soil", *Soils Found.*, **29**(1), 82-92. https://doi.org/10.3208/sandf1972.29.82.

Liang, F.Y. and Song, Z. (2014), "BEM analysis of the interaction factor for vertically loaded dissimilar piles in saturated poroelastic soil", *Comput. Geotech.*, **62**, 223-231. https://doi.org/10.1016/j.compgeo.2014.07.016

Liang, F.Y., Chen, L.Z. and Han, J. (2009), "Integral equation method for analysis of piled rafts with dissimilar piles under vertical loading", *Comput. Geotech.*, **36**(3), 419-426. https://doi.org/10.1016/j.compgeo.2008.08.007.

Ma, Q., Mou, J. and Xiao, H.L. (2021), "Experimental and numerical studies on bearing characteristics of hexagonal-section composite foundation element", *Iranian J. Sci. Tech. T. Civil Eng.*, **45**(2), 929-939. https://doi.org/10.1007/s40996-020-00389-7.

Mindlin, R.D. (1936), "Force at a point in the interior of a semi-infinite solid", *Physics*, **7**(5), 195-202. https://doi.org/10.1063/1.1745385.

Ministry of Housing and Urban-Rural Development of the People's Republic of China[S]. Beijing, China Architecture Publishing

Ministry of Housing and Urban-Rural Development of the People's Republic of China [S]. Beijing, China Architecture Publishing.

Muki, R. and Sternberg, E. (1970), "Elastostatic load-transfer to a half-space from a partially embedded axially loaded rod", *Int. J. Solids Struct.*, **6**(1), 69-90. https://doi.org/10.1016/0020-7683(70)90082-X.

Poulos, H.G. (1967), "Stresses and displacements in an elastic layer underlain by a rough rigid base", *Geotechnique*, **17**(4), 378-410. https://doi.org/https://doi.org/10.1680/geot.1967.17.4.378.

Poulos, H.G. and Davis, E.H. (1980), Pile foundation analysis and design.

Qu, L.M., Ding, X.M., Zheng, C.J., Wu, C. and Cao, G. (2021), "Numerical and test study on vertical vibration characteristics of pile group in slope soil topography", *Earthq. Eng. Eng. Vib.*, **20**(2), 377-390. https://doi.org/10.1007/s11803-021-2026-7.

Randolph, M.F. and Wroth, C.P. (1979), "An analysis of the vertical deformation of pile groups", **29**(4), 423-439. https://doi.org/10.1680/geot.1979.29.4.423.

Roh, Y., Kim, G., Kim, I. and Lee, J. (2019), "Effects of rock-support and inclined-layer conditions on load carrying behavior of piled rafts", *Geomech. Eng.*, **18**(4), 363-371. https://doi.org/10.12989/gae.2019.18.4.363.

Saeedi Azizkandi, A., Rasouli, H. and Baziar, M.H. (2018), "Load sharing and carrying mechanism of piles in non-connected pile rafts using a numerical approach", *Int. J. Civil Eng.*, **17**(6), 793-808. https://doi.org/10.1007/s40999-018-0356-2.

Shen, W.Y., Chow, Y.K. and Yong, K.Y. (1999), "Variational solution for vertically loaded pile groups in an elastic half-space", *Geotechnique*, **49**(2), 199-213. https://doi.org/https://doi.org/10.1680/geot.1999.49.2.199.

Shen, W.Y., Chow, Y.K. and Yong, K.Y. (2000), "A variational approach for the analysis of pile group–pile cap interaction", *Geotechnique*, **50**(4), 349-357. https://doi.org/https://doi.org/10.1680/geot.2000.50.4.349.

Wong, S.C. and Poulos, H.G. (2005), "Approximate pile-to-pile interaction factors between two dissimilar piles", *Comput. Geotech.*, **32**(8), 613-618. https://doi.org/https://doi.org/10.1016/j.compgeo.2005.11.001.

Yang, M.H., Zhang, X.W. and Zhao, M.H. (2011), "A simplified approach for settlement calculation of pile groups considering pile-to-pile interaction in layered soils", *J. Central South Univ. Technol.*, **18**(6), 2131-2136. https://doi.org/10.1007/s11771-011-0953-6

Yu, J.L., Zhou, J.J., Gong, X.N., Xu, R.Q., Li, J.Y., Xu, S.D. (2020), "Centrifuge study on behavior of rigid pile composite foundation under embankment in soft soil", *Acta Geotechnica*, **16**(6), 1909-1921. https://doi.org/10.1007/s11440-020-01109-1.

Zhang, D.M., Huang, Z.K., Wang, R.L., Yan, J.Y. and Zhang, J. (2018), "Grouting-based treatment of tunnel settlement: Practice in Shanghai", *Tunn. Undergr. Sp. Tech.*, **80**, 181-196. https://doi.org/10.1016/j.tust.2018.06.017.

Zhang, Z.T., Gong, W.M., DaiG.L., Cao, X.L., Zhu, Y. and Huang, H. (2021), "Field tests on bearing characteristics of large-diameter combined tip-and-side post grouted drilled shafts", *Appl. Sci.*, **11**(24), https://doi.org/10.3390/app112411883.

GC